Postnatal synaptic potentiation: Delivery of GluR4-containing AMPA receptors by spontaneous activity

J. Julius Zhu[1], José A. Esteban[1], Yasunori Hayashi[2] and Roberto Malinow[1]

[1] *Cold Spring Harbor Laboratory, 1 Bungtown Road, Cold Spring Harbor, New York 11724, USA*

[2] *Center for Learning and Memory, Massachusetts Institute of Technology, Cambridge, Massachusetts 02139, USA*

The first two authors contributed equally to this work

Correspondence should be addressed to R.M. (malinow@cshl.org)

To examine how functional circuits are established in the brain, we studied excitatory transmission in early postnatal hippocampus. Spontaneous neural activity was sufficient to selectively deliver GluR4-containing AMPA receptors (AMPA-Rs) into synapses. This delivery allowed non-functional connections to transmit at resting potentials and required NMDA receptors (NMDA-Rs) but not CaMKII activation. Subsequently, these delivered receptors were exchanged with non-synaptic GluR2-containing AMPA-Rs in a manner requiring little neuronal activity. The enhanced transmission resulting from this delivery and subsequent exchange was maintained for at least several days and required an interaction between GluR2 and NSF. Thus, this sequence of subunit-specific trafficking events triggered by spontaneous activity in early postnatal development may be crucial for initial establishment of long-lasting functional circuitry.

The proper formation of synaptic circuits is an outstanding biological problem[1]. It is believed that the construction of functional neuronal circuits requires two general processes[2]. The initial rough neuronal connectivity diagram is established through multiple interactions among extending axons and surface molecules on the target tissue; this process may not require neuronal electrical activity. Once axons have been guided to regions by such surface cues, synapses are made on postsynaptic neurons. Narp[3] and neuroligin[4] are candidate molecules proposed to trigger this initial synapse formation. After these initial events, synapses are extensively remodeled to establish precise functional connections, and neuronal activity seems to be crucial in this process[5]. Here we try to understand this activity-dependent aspect of circuit formation.

Excitatory synaptic transmission in mature neurons is mediated by the actions of glutamate, on two different ion-permeable receptors, NMDA-Rs and AMPA-Rs[6]. In contrast to AMPA-Rs, NMDA-Rs require membrane depolarization to transmit and are largely inactive at resting membrane potentials. Excitatory synaptic contacts initially contain primarily NMDA-Rs[7,8] and are electrophysiologically 'silent' at normal resting potentials[9–11]. Such synapses must acquire AMPA-Rs to form connections that can function in the absence of concomitant depolarizing input. It is not known how initially formed synapses acquire AMPA-Rs.

Studies examining long-term potentiation (LTP) suggest that rapid trafficking of AMPA-Rs from non-synaptic to synaptic regions may contribute to this form of activity-induced synaptic enhancement[12,13]. In particular, AMPA-Rs containing the AMPA-R subunit GluR1 seem to be driven to synapses by a mechanism triggered by activation of calcium/calmodulin-dependent protein kinase II (CaMKII). The proper delivery of these AMPA-Rs requires an interaction between GluR1 and PDZ domain protein(s). There are several parallels between LTP and synaptic maturation[14], and thus it is reasonable to examine if the receptor trafficking identified in LTP also is involved in synaptic maturation.

A question regarding receptor trafficking is whether a rapid transient delivery of receptors to synapses, as may occur during plasticity, leads to a long-lasting increase in the number of receptors at those synapses. If this happens, there must be mechanisms by which the delivered receptors are replaced in a way that maintains the 'memory' of their delivery. Recent evidence suggests that rapid cycling of receptors depends on interactions between the AMPA-R subunit GluR2 and NSF[15–19]. To determine the relationship between the transient delivery during plasticity and this receptor cycling, we examined the cellular and molecular aspects of synaptic physiology during the early postnatal development of the hippocampus.

Results

The developmental profile of AMPA receptor subunits in hippocampus was assayed by western immunoblots using subunit-specific antibodies (Methods; Fig. 1a). Although GluR1, GluR2 and GluR2/3 levels increased gradually during development and stabilized at 20 days of age, GluR4 expression was largely restricted to the first postnatal week. These immunoblots did not give information regarding the relative amount of different subunits (for example, the amount of GluR4 relative to GluR1) because subunit-specific antibodies may label their targets to different degrees. To determine the relative amount of each subunit, we determined the relative labeling efficiency of each subunit-specific antibody. We did this by expressing GFP-tagged cytoplasmic tails of each subunit in hippocampal slices using the Sindbis expression system[20]. These constructs could be detected by subunit-specific antibodies and the anti-GFP antibody. (We tested both monoclonal and polyclonal

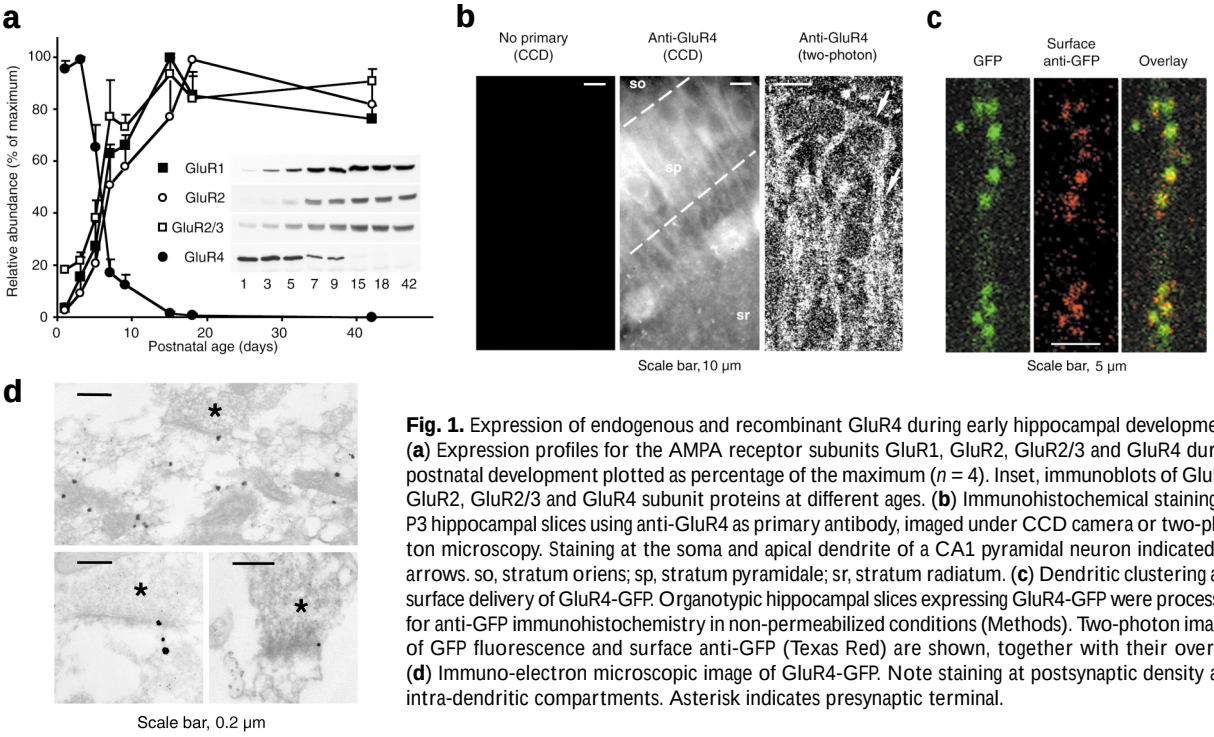

Fig. 1. Expression of endogenous and recombinant GluR4 during early hippocampal development. (**a**) Expression profiles for the AMPA receptor subunits GluR1, GluR2, GluR2/3 and GluR4 during postnatal development plotted as percentage of the maximum ($n = 4$). Inset, immunoblots of GluR1, GluR2, GluR2/3 and GluR4 subunit proteins at different ages. (**b**) Immunohistochemical staining of P3 hippocampal slices using anti-GluR4 as primary antibody, imaged under CCD camera or two-photon microscopy. Staining at the soma and apical dendrite of a CA1 pyramidal neuron indicated by arrows. so, stratum oriens; sp, stratum pyramidale; sr, stratum radiatum. (**c**) Dendritic clustering and surface delivery of GluR4-GFP. Organotypic hippocampal slices expressing GluR4-GFP were processed for anti-GFP immunohistochemistry in non-permeabilized conditions (Methods). Two-photon images of GFP fluorescence and surface anti-GFP (Texas Red) are shown, together with their overlay. (**d**) Immuno-electron microscopic image of GluR4-GFP. Note staining at postsynaptic density and intra-dendritic compartments. Asterisk indicates presynaptic terminal.

anti-GFP antibodies.) These constructs could thus be used to determine the labeling efficiency of the subunit-specific cytoplasmic tail antibodies. (For original data, see supplementary figure.) Using this method, we determined the relative amounts of the AMPA-R subunits GluR1, GluR2 and GluR4. This analysis indicates that, whereas GluR4 is mostly expressed early in development, at P2, the absolute levels of GluR1, GluR2 and GluR4 are similar. To determine which cells express GluR4 early in development, we used immunohistochemistry. At this early stage, pyramidal cells expressed GluR4 (Fig. 1b).

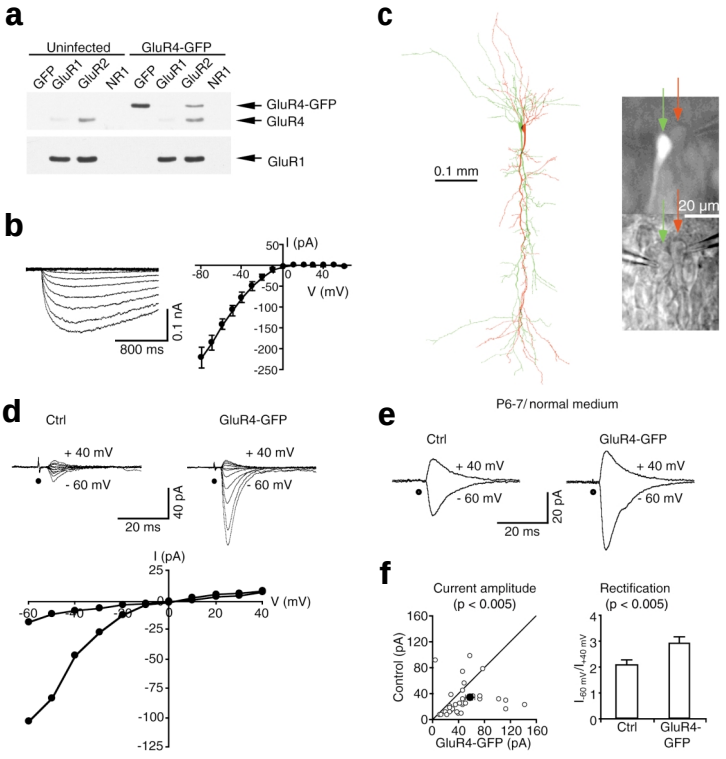

Fig. 2. Synaptic delivery of recombinant GluR4. (**a**) Co-immunoprecipitation of GluR4-GFP with endogenous AMPA receptors. Immunoprecipitation on uninfected or GluR4-GFP-expressing slices as done with antibodies shown at a slant. Most GluR4-GFP (81.5 ± 6%, $n = 3$) is not associated with GluR2. (**b**) Current–voltage plot of whole-cell responses of HEK 293 cells transfected with GluR4-GFP ($n = 4$). (**c**) Left, camera lucida reconstruction of control uninfected and infected CA1 cells filled with biocytin. Right, uninfected CA1 and infected cells under fluorescence (top) and transmitted (bottom) light microscopy. (**d**) Simultaneous evoked AMPA-R-mediated responses (each trace, average of 20 trials) from uninfected (ctrl) and infected (GluR4-GFP) cells. GluR4-GFP was expressed in cultured slices in normal culture medium (Methods) for 36 hours. The membrane potentials were clamped at –60 mV to +40 mV, at 10 mV steps. Current–voltage plot of synaptic responses simultaneously recorded from control and infected cells. Stimulation artifacts are marked by filled circles. (**e**) Example of averaged responses from control and cell infected with GluR4-GFP recorded at –60 mV and +40 mV, as indicated. (**f**) Left, amplitude of synaptic AMPA-R-mediated responses (at –60 mV) of control uninfected cells are plotted against those obtained from infected cells; filled circle shows averages (infected, –56.8 ± 7.6 pA; ctrl, –32.6 ± 4.5 pA; $n = 34$; $p < 0.005$). For reference, $x = y$ line. Right, rectification ($I_{-60\ mV}/I_{+40\ mV}$) of the same cells (infected, 2.91 ± 0.26; ctrl, 2.03 ± 0.14; $n = 34$; $p < 0.005$).

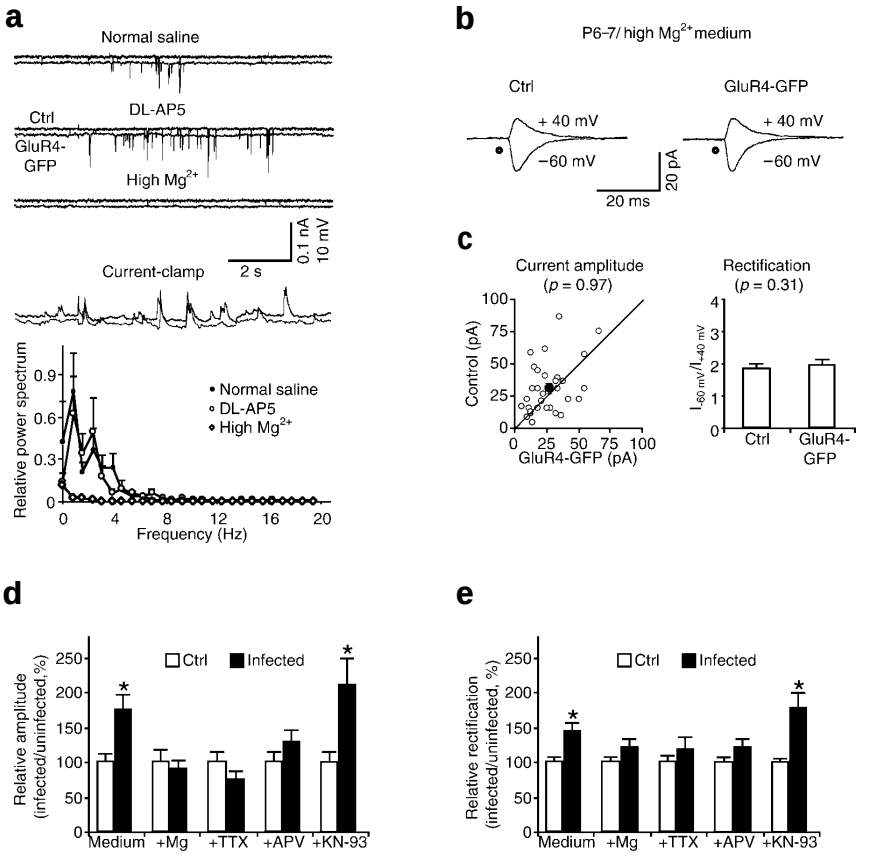

Fig. 3. Spontaneous activity delivers GluR4-GFP into synapses. (**a**) Spontaneous, periodic synaptic activity (at approximately 0.001–0.1 Hz) in uninfected cell (top traces) and infected cell (bottom traces) appears as clusters of large EPSCs in voltage-clamp mode. Such activity is insensitive to bath application of 100 μM D,L-APV, but is completely blocked by bath application of 12 mM Mg^{2+}. In current-clamp mode, the activity is represented as intermittent fluctuations of membrane potential that is little affected by D,L-APV, but largely suppressed by 12 mM Mg^{2+}. Bottom, relative power spectrum of spontaneous activity in normal saline (ctrl), D,L-APV or 12 mM Mg^{2+} is recorded as indicated. (**b**) Synaptic AMPA-R-mediated responses from nearby uninfected and infected cells after GluR4-GFP expression in high Mg^{2+} culture medium. (**c**) Left, amplitude of synaptic AMPA-R-mediated responses (at –60 mV) of control uninfected cells are plotted against those obtained from infected cells. Right, rectification ($I_{-60\ mV}/I_{+40\ mV}$) of the same cells (n = 32). (**d**, **e**) AMPA-R-mediated current amplitude (**d**) and rectification (**e**) in cells expressing GluR4-GFP relative to uninfected neighboring control cells. Values for slices maintained in control (normal medium; values given in **Fig. 2f**) or with 12 mM Mg^{2+} (infected, –26.2 ± 3.4 pA; ctrl, –28.9 ± 5.5 pA; n = 20; p = 0.97 for amplitude; infected, 2.32 ± 0.28; ctrl, 1.94 ± 0.16; n = 20; p = 0.31 for rectification) or 1 μM TTX (infected, –33.0 ± 6.9 pA; ctrl, –44.1 ± 5.1 pA; n = 14; p = 0.17 for amplitude; infected, 2.13 ± 0.29; ctrl, 1.79 ± 0.20; n = 14; p = 0.13 for rectification), or 100 μM D,L-APV (infected, –53.4 ± 9.2 pA; ctrl, –43.1 ± 8.7 pA; n = 20; p = 0.19 for amplitude; infected, 2.31 ± 0.20; ctrl, 1.89 ± 0.13; n = 20; p = 0.07 for rectification) or 20 μM KN-93 (infected, –52.3 ± 9.1 pA; ctrl, –24.7 ± 3.9 pA; n = 24; p < 0.01 for amplitude; infected, 3.53 ± 0.44; ctrl, 1.99 ± 0.12; n = 24; p < 0.005 for rectification). AMPA-R mediated current amplitude, rectification and standard errors were normalized to average current and rectification values from control cells for (**d**) and (**e**). Asterisk indicates p < 0.05 (Wilcoxon test).

To examine the potential role of GluR4 in synaptic plasticity during this early period, we expressed[20] GluR4 tagged with GFP (GluR4-GFP) in hippocampal slices obtained from P5–7 animals. Approximately 36 hours after expression, GluR4-GFP appeared clustered in dendrites, with some delivery to the surface (Fig. 1c). Electron microscopy indicated that GluR4-GFP was delivered to dendrites, and some reached synaptic sites (Fig. 1d).

To study the regulation of GluR4-GFP delivery to synapses, we used electrophysiological tagging[13]. GluR4-GFP expressed in CA1 cells mainly formed receptors lacking GluR2 subunits (Fig. 2a); these receptors show inward rectification[21] (Fig. 2b). Because AMPA-receptor-mediated transmission in pyramidal neurons is largely non-rectifying[22] (Fig. 2e, left; and f, right), delivery of recombinant receptors can be detected by an increased rectification of synaptic responses[13]. By comparing transmission simultaneously evoked onto pairs of nearby infected and non-infected neurons (Fig. 2c–f), we found that responses in cells expressing GluR4-GFP had both larger amplitudes at –60 mV and greater rectification, indicating synaptic delivery of homomeric GluR4-GFP receptors.

Recordings from CA1 neurons demonstrated intermittent synaptic activity[23–25] (Fig. 3a) that could be blocked by addition of high Mg^{2+} (n = 16; Fig. 3a) or TTX (n = 8; data not shown) in the bath. To determine if this activity is required to deliver receptors to synapses, we infected slices with GluR4-GFP and immediately exposed them to high Mg^{2+} or TTX. Thirty-six hours after expression in slices whose activity was blocked, GluR4-GFP distribution in dendritic regions was largely unchanged. As detected with two-photon laser scanning microscopy, dendrites still showed fluorescence, and the fraction of GluR4-GFP in clusters remained similar (0.38 ± 0.05 in normal medium, and 0.29 ± 0.06 in high Mg^{2+}; n = 16; t-test, p = 0.16; Methods). However, synaptic delivery was blocked. Transmission onto infected cells was not different from transmission onto neighboring non-infected control cells, with respect to amplitude and rectification (Fig. 3b–e). To test whether this activity-dependent delivery of GluR4-GFP required NMDA receptor activation, we incubated slices in APV during the expression of GluR4-GFP. Although spontaneous activity was not blocked (n = 6; Fig. 3a), synaptic delivery of the receptor was largely attenuated (Fig. 3d and e). Because synaptic delivery of GluR4-GFP required NMDA receptor activation, we then examined whether this process requires CaMKII activation using the drug KN-93, a membrane-permeable CaMKII inhibitor[26] that blocked LTP (tested in P12 slices, n = 4; data not shown). In slices maintained in the presence of KN-93 (20 μM), transmission onto cells expressing GluR4-GFP was still enhanced and was more rectified (Fig. 3d and e). This indicates that, in con-

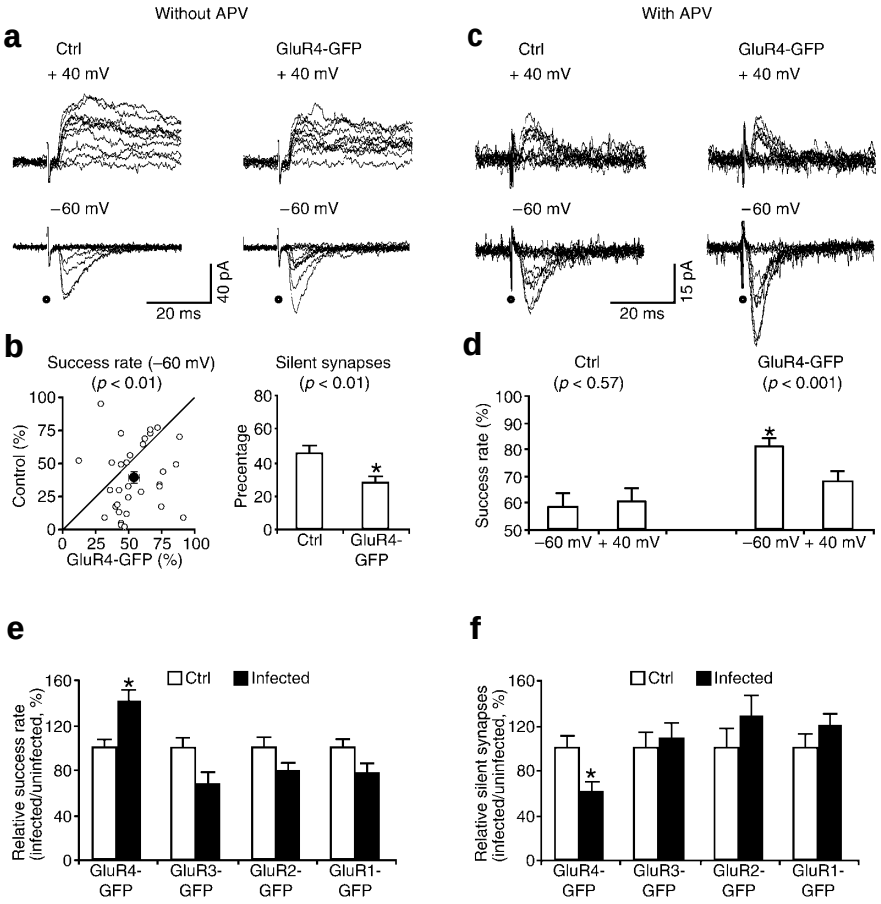

Fig. 4. Delivery of GluR4-GFP to silent synapses. (**a**) Consecutive evoked synaptic responses recorded at +40 mV and –60 mV from an uninfected control and a neighboring infected (GluR4-GFP) cell. (**b**) Left, transmission success rates of control (uninfected) cells are plotted against those obtained from nearby infected cells. Right, fraction of silent synapses estimated for the same cells (infected, 27.6 ± 4.1%; ctrl, 45.1 ± 5.2%; $n = 23$; $p < 0.01$). (**c**) Consecutive evoked synaptic AMPA-R-mediated responses (in APV) recorded at +40 mV and –60 mV from a nearby pair of uninfected control and infected cells. (**d**) The transmission success rates of control uninfected and infected cells recorded in APV are significantly higher in infected cells at –60 mV (infected, 81.1 ± 2.8%; ctrl, 58.1 ± 5.7%; $n = 24$; $p < 0.001$), but are comparable at +40 mV (infected, 68.0 ± 3.9%; ctrl, 60.3 ± 5.8%; $n = 24$; $p = 0.57$). Synaptic transmission success rate (**e**) and fraction of silent synapses (**f**) in cells expressing GluR4-GFP, GluR3-GFP (infected, 63.7 ± 5.5%; ctrl, 42.6 ± 7.0%; $n = 20$; $p = 0.07$ for success rate; infected, 45.1 ± 6.2%; ctrl, 41.7 ± 5.8%; $n = 20$; $p = 0.54$ for silent synapses), GluR2-GFP (infected, 41.5 ± 4.0%; ctrl, 52.4 ± 5.3%; $n = 20$; $p = 0.13$ for success rate; infected, 38.1 ± 5.8%; ctrl, 29.9 ± 5.1%; $n = 20$; $p = 0.20$ for silent synapses) or GluR1-GFP (infected, 43.9 ± 5.8%; ctrl, 57.1 ± 4.4%; $n = 20$; $p = 0.13$ for success rate; infected, 49.1 ± 4.9%; ctrl, 41.1 ± 5.2%; $n = 20$; $p = 0.33$ for silent synapses), compared to uninfected controls. Values from groups were averaged and then normalized to average current and rectification values from uninfected controls. Asterisk indicates $p < 0.05$ (Wilcoxon test).

trast to LTP in mature animals[27], CaMKII activation is not required for synaptic delivery of this receptor.

Early in postnatal development, a large fraction of excitatory synapses produce only NMDA-receptor-mediated responses[9–11,28]. Such synapses produce no response at resting membrane potentials, and therefore have been termed 'silent' synapses[29]. To determine whether GluR4-GFP is delivered to such synapses, we measured the response success rate (fraction of successful responses) on nearby infected and non-infected cells. Evoked transmission onto cells expressing GluR4-GFP showed a greater success rate when cells were clamped at the normal resting potential (infected, 54.4 ± 4.6%; control, 38.9 ± 3.2%; $n = 32$; $p < 0.01$), but not when clamped at depolarized potential (infected, 60.3 ± 4.5%; ctrl, 58.0 ± 5.6%; $n = 23$; $p = 0.68$; Fig. 4a and b, left). These data indicated that these cells had fewer silent synapses (Fig. 4b, right). To test whether GluR4-GFP homomeric receptors were delivered to synapses lacking endogenous (non-rectifying) AMPA receptors, we took advantage of the rectification of GluR4 homomeric receptors. We measured success rate at hyperpolarized and depolarized potentials in the presence of APV (to block NMDA-receptor-mediated responses). As previously shown[29], success rates at hyperpolarized and depolarized potentials were similar in non-infected cells when measured in the presence of APV (Fig. 4c and d). However, in cells expressing GluR4-GFP, there were significantly more successes at hyperpolarized potentials compared to depolarized potentials (Fig. 4c and d). These data indicated that cells expressing GluR4-GFP, have a significant fraction of synapses containing only rectifying AMPA receptors, which suggested that GluR4-GFP is delivered to synapses that do not have endogenous AMPA receptors (silent synapses). GluR1-GF, which can be delivered to synapses by LTP[13], was not delivered to synapses by spontaneous activity (Fig. 4e). Neither success rate at hyperpolarized potentials nor fraction of silent synapses changed in infected cells (Fig. 4e and f). Similar results were found for cells infected with GluR2-GFP and GluR3-GFP (Fig. 4e and f). These results indicated that spontaneous activity specifically promotes the synaptic delivery of GluR4-GFP, converting silent synapses into functional ones at early stages of circuit formation.

We next wanted to test if endogenous GluR4-containing AMPARs are delivered to synapses by activity. Because synaptic trafficking of glutamate receptors seems to be controlled mainly by interactions mediated by their cytoplasmic tail[30], overexpression of the cytoplasmic tail would be expected to block such interactions and therefore interfere with synaptic delivery. Cells expressing the GluR4 cytoplasmic tail (GluR4ct-GFP) for 36 hours showed markedly decreased transmission relative to nearby uninfected cells

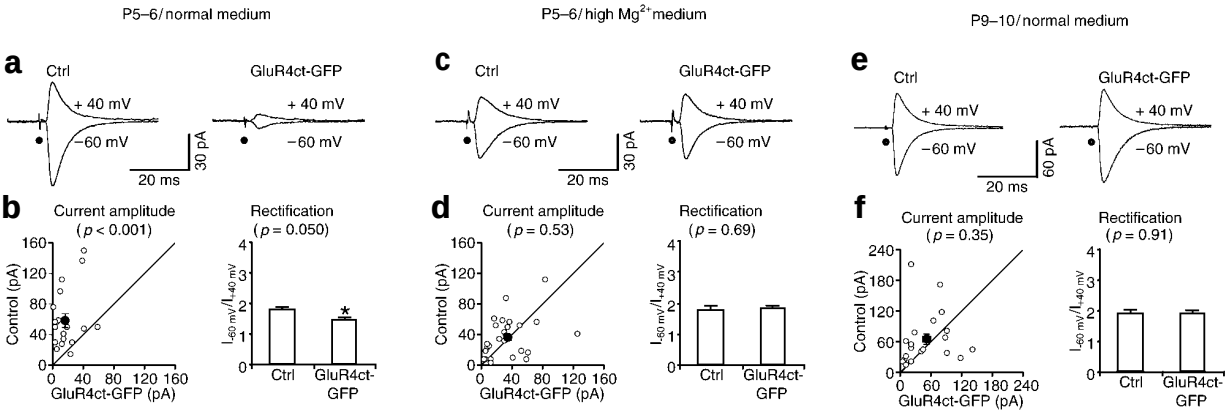

Fig. 5. Delivery of endogenous GluR4 into synapses. (**a**) Synaptic AMPA-R-mediated responses from a pair of cells, one uninfected (left) and the other infected with GluR4ct-GFP (right). (**b**) Left, synaptic AMPA-R-mediated responses (at –60 mV) of control uninfected and infected cells plotted against each other (infected, –18.3 ± 3.6 pA; ctrl, –56.9 ± 8.9 pA; n = 20; p < 0.001). Right, rectification ($I_{-60\ mV}/I_{+40\ mV}$) of the same cells (infected, 1.45 ± 0.14; ctrl, 1.77 ± 0.15; n = 20; p = 0.050). (**c**, **d**) Synaptic AMPA-R-mediated responses (infected, –35.3 ± 5.7 pA; ctrl, –35.7 ± 5.2 pA; n = 26; p = 0.53) and rectification (infected, 1.82 ± 0.12; ctrl, 1.77 ± 0.14; n = 26; p = 0.69) are comparable in infected and control uninfected cells in slices maintained with 12 mM Mg^{2+} during expression. (**e**, **f**) Synaptic AMPA-R-mediated responses (infected, –51.9 ± 9.1 pA; ctrl, –63.8 ± 11.5 pA., n = 20; p = 0.35) and rectification (infected, 1.87 ± 0.14; ctrl, 1.80 ± 0.15; n = 20; p = 0.91) are also comparable in infected and control uninfected cells from P9–10 animals maintained in normal medium.

(Fig. 5a and b). This decrease was accompanied by a decrease in success rate (infected, 72.6 ± 4.5; ctrl, 97.6 ± 1.0; n = 20, p < 0.001), suggesting that delivery of endogenous GluR4-containing receptors to silent synapses was blocked by GluR4ct-GFP. Cells expressing GluR4ct-GFP had a slightly lower rectification than control cells (Fig. 5b), suggesting that some of the synaptically delivered endogenous receptors may be rectifying (that is, lacking GluR2). If synaptic delivery of endogenous GluR4-containing receptors is mediated by spontaneous activity, then overexpression of GluR4ct-GFP should have no effect on slices maintained with activity blocked. Indeed, in slices that had been incubated in high Mg^{2+}, cells expressing GluR4ct-GFP for 36 hours had transmission indistinguishable from nearby uninfected cells (Fig. 5c and d). As a further test for the specificity of this construct, we expressed GluR4ct-GFP in slices prepared from P9–10 animals. At this age, there is little endogenous GluR4 (Fig. 1a). Transmission onto cells from P9–10 animals expressing GluR4ct-GFP for 36 hours was similar to transmission from nearby non-infected cells, with respect to amplitude and rectification (Fig. 5e and f). These results indicate that GluR4ct-GFP depresses synaptic transmission specifically by blocking activity-dependent delivery of endogenous GluR4-containing AMPA receptors. To further examine whether spontaneous activity promotes delivery of endogenous AMPA receptors, we tested the effects of incubation with high Mg^{2+} on the ratio of AMPA to NMDA receptor-mediated responses. Consistent with the prediction that activity drives endogenous AMPA receptors to synapses, slices incubated in high Mg^{2+} for 36 hours had a significantly lower ratio of AMPA to NMDA receptor-mediated responses when compared to slices incubated in control medium (0.36 ± 0.04; n = 23 versus 1.55 ± 0.19 n = 20; t-test, p < 0.0001).

To determine the long-term fate of GluR4-containing AMPA receptors after delivery to synapses by spontaneous activity, we conducted the following experiment. Slices were prepared, and expression of GluR4-GFP was allowed to proceed with normal spontaneous activity to drive the synaptic incorporation of the recombinant protein. Thirty-six hours later, high Mg^{2+} was added, which should have blocked any subsequent synaptic delivery of GluR4. Transmission was then examined for the next several days. Transmission onto cells expressing GluR4-GFP was still enhanced for several days after activity was blocked (Fig. 6). This enhanced transmission no longer showed the increased rectification characteristic of GluR4-GFP-containing receptors. This indicates that endogenous AMPA receptors containing GluR2 (non-rectifying receptors[21]) have replaced the rectifying recombinant synaptic receptors. Indeed, we found evidence for endogenous GluR2-containing AMPA-Rs replacing endogenous GluR2-lacking AMPA-Rs. The existence of endogenous GluR2-lacking AMPA-Rs was supported by co-immunoprecipitation. Early in development, a significant fraction of GluR4-containing AMPA-Rs lack GluR2 (approximately 70% at P2, approximately 25% at P6). Endogenous AMPA-Rs containing GluR4 (and lacking GluR2) may be delivered to synapses in an activity-dependent manner (Fig. 5b, right). However, the expression of endogenous GluR2-containing receptors, even in early development, may be high enough to efficiently replace these rectifying receptors. This is indicated by the constant and relative lack of rectification observed at different times in development (rectification at P3, 1.80 ± 0.17, n = 18; at P12, 1.64 ± 0.14, n = 18; t-test, p = 0.45; recorded from CA1 pyramidal neurons in acute slices).

What is the mechanism underlying this replacement? Studies suggest that a pool of AMPA receptors can cycle between synaptic and non-synaptic sites[15–19]. This cycling depends on interactions between GluR2 and NSF, and can be prevented by a peptide (pep2m/G10) containing the NSF-interacting region of GluR2. To test whether such interactions are involved in the plasticity we characterized in this study, we infected slices with GluR4-GFP and allowed 36 hours of spontaneous activity to deliver the recombinant receptor to synapses. At this point, intracellular loading of pep2m/G10 decreased transmission markedly in control cells but had diminished effects on GluR4-GFP-expressing cells (Fig. 7a–c). Furthermore, the decrease of transmission in infected cells was accompanied by an additional increase in rectification

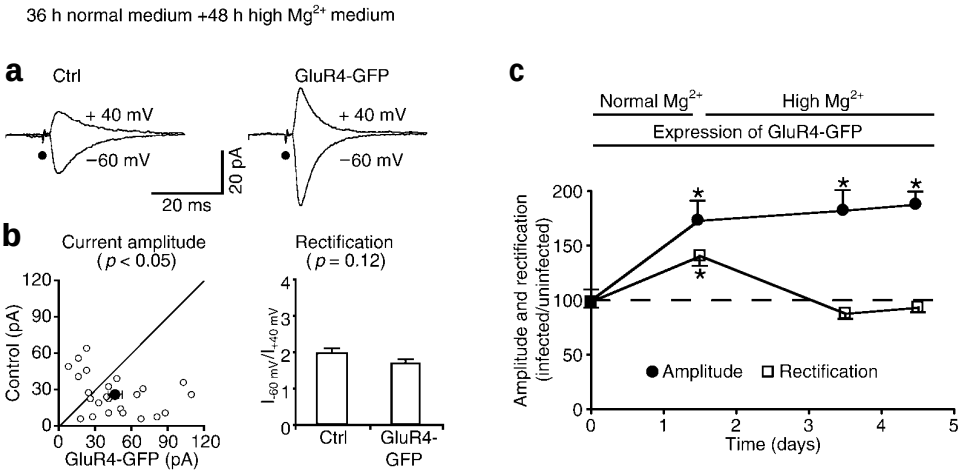

Fig. 6. Exchange of synaptic GluR4-GFP with endogenous GluR2-containing receptor maintains potentiated transmission. (**a**) Synaptic AMPA-R-mediated responses from a pair of uninfected and infected cells after expression of GluR4-GFP in normal culture medium for 36 hours followed by high Mg^{2+} culture medium for an additional 48 hours. (**b**) Left, synaptic AMPA-R-mediated response amplitudes (at –60 mV) of control uninfected cells are plotted against those obtained from infected cells. Right, bar graph showing rectification ($I_{-60\ mV}/I_{+40\ mV}$) of the same cells (n = 24). (**c**) Plot of AMPA-R-mediated responses in GluR4-GFP infected relative to controls uninfected cells plotted against the expression time. Amplitude (infected, –47.0 ± 5.7 pA; ctrl, –25.5 ± 3.4 pA; n = 24; $p < 0.05$ for day 3.5; infected, –37.6 ± 4.4 pA; ctrl, –20.0 ± 2.9 pA; n = 22; $p < 0.005$ for day 4.5) and rectification (infected, 1.69 ± 0.10; ctrl, 1.92 ± 0.12; n = 24; $p = 0.12$ for day 3.5; infected, 1.51 ± 0.07; ctrl, 1.61 ± 0.10; n = 22; $p = 0.58$ for day 4.5). Values for each group were averaged and normalized to average current and rectification values obtained from uninfected groups. Asterisk indicates $p < 0.05$ (Wilcoxon).

(4.66 ± 0.97, n = 10 versus 2.91 ± 0.26, n = 34; t-test, $p < 0.05$; comparison with infected cells not infused with pep2m/G10, Fig. 2f). These results indicate that the enhanced transmission produced by delivery of GluR4-GFP does not require GluR2-NSF interactions initially. However, once the delivered GluR4-GFP is replaced by GluR2-containing receptors, the long-term maintenance of the enhanced transmission may involve receptor cycling that requires GluR2-NSF interactions. We thus tested the effects of pep2m/G10 on cells expressing GluR4-GFP that had been exposed to normal Mg^{2+} for 36 hours, followed by exposure to high Mg^{2+} for another 48–72 hours. In this case, the peptide had similar effects on infected and control cells (Fig. 7d–f). Indeed, the fractional block of transmission by pep2m/G10 for 36 hours was significantly different from exposure for 48–72 hours after GluR4-GFP delivery (ratio of residual current of infected to residual current of uninfected cells: $R_{36\ h}$ = 1.71 ± 0.19, n = 10; $R_{48–72\ h}$ = 1.16 ± 0.14, n = 12; t-test, $p < 0.05$). Thus, an interaction between GluR2 and NSF seems to be involved in the maintenance of the enhanced transmission, but not in the initial delivery.

Discussion

The mechanisms that promote the formation of functional neuronal circuits are poorly understood, although spontaneous neuronal activity is thought to have an important role[14,31,32]. Most excitatory synapses initially have only NMDA receptors[7–11,28,33], and such synapses transmit little electrophysiological information at resting membrane potentials[29,34]. During development, these synapses acquire AMPA receptors; such synapses can transmit faithfully. What mechanisms drive this functional transformation? Here we show that spontaneous activity, which can be recorded early in hippocampus[23–25] and other developing tissue[35,36], is sufficient to trigger a long-lasting enhancement of synaptic transmission by delivering AMPA receptors to synapses, including silent synapses. Furthermore, we identify GluR4 as the AMPA receptor subunit mediating this delivery during the early postnatal development of the hippocampus.

The synaptic plasticity occurring in older animals that may be involved in learning and memory (for example, LTP[37]) may also be responsible for developmental plasticity. Here we show that these two forms of plasticity have some similarities and differences. Both processes involve the activity-driven delivery of AMPA receptors. However, early in development, spontaneous activity delivers GluR4 independently from CaMKII activity, whereas later in development, GluR1 is delivered[12,38] in a CaMKII-dependent manner[13] that cannot be triggered by low-frequency spontaneous activity alone. Thus, plasticity at different developmental stages may be adapted to the different patterns and levels of neuronal activity likely to be present at different ages.

The effect of spontaneous activity on synaptic function has been studied with cultured dissociated cell preparations[39–42]. Although some results are in agreement with those presented here, other reports show that manipulations on activity can have effects opposite from ours. This conflict may be related to culture conditions, duration of manipulations, and differences between cultured dissociated preparations and cultured slices. In particular, there seem to be differences between dissociated cultured neurons and cultured slices with respect to AMPA receptor trafficking (GluR1 is delivered constitutively to synapses in dissociated cells but not in cultured slices[12]) and synaptic plasticity (LTP is rarely seen in dissociated cells but is prominent in cultured slices[43]).

An issue concerning the construction of neuronal circuits is how altered synaptic connections are preserved in the face of protein turnover. In particular, how is the strength of potentiated synapses maintained? Here we find that synapses potentiated by transient delivery of GluR4-containing AMPA receptors maintain their strength over the course of (at least) the next several days. Furthermore, whereas activity is necessary to trigger enhanced strength, its long-term maintenance is apparently due to the exchange of synaptic receptors with endogenous receptors containing GluR2 in an activity-independent manner. (In other synapses, this exchange may require activity[44].) Finally, whereas an interaction between GluR2 and NSF is not required for the initial stages of enhanced strength, this interaction is required to maintain enhanced strength

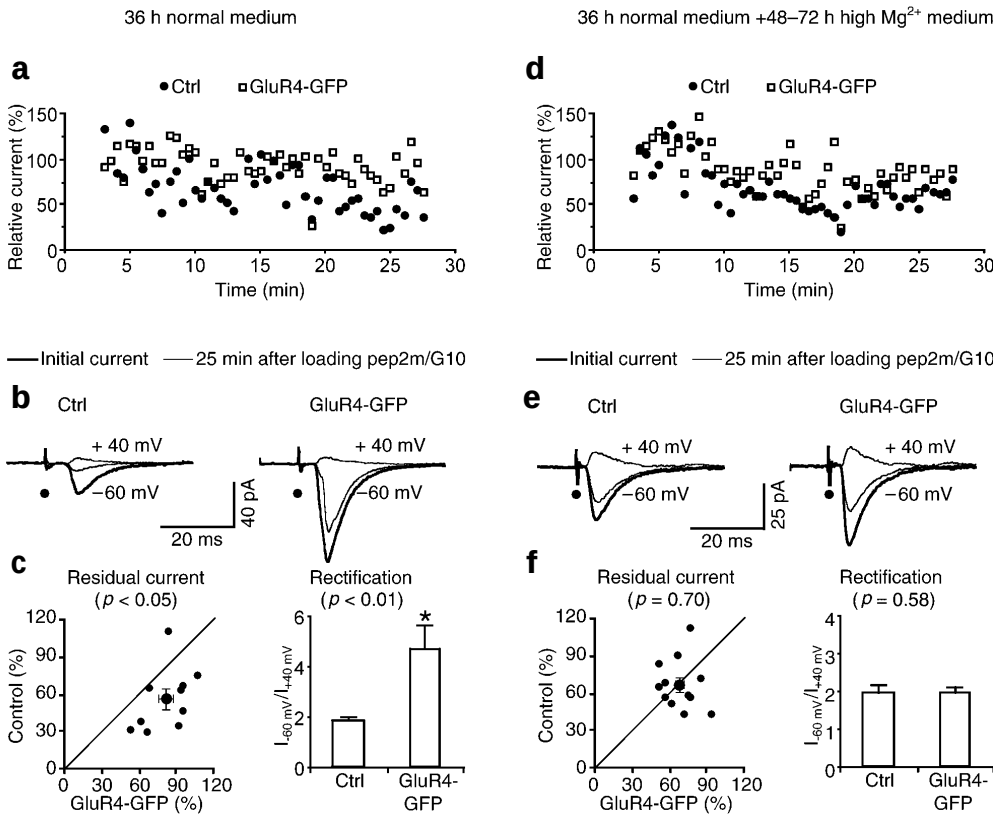

Fig. 7. Maintenance of enhanced transmission depends on interactions between GluR2 and NSF. (**a**) Normalized simultaneously evoked responses from cells expressing or not expressing GluR4-GFP versus the time after forming whole-cell configuration. Experiment was conducted after slices were infected and maintained in normal medium for 36 hours. (**b**) Average AMPA-R-mediated synaptic responses obtained immediately (–60 mV, thick trace) and 25 minutes after whole-cell infusion of pep2m/G10 (–60 mV and +40 mV, thin trace) from a pair of infected (GluR4-GFP) and uninfected cells. After infection, slices were kept in normal culture medium for 36 hours. (**c**) Left, residual synaptic AMPA-R-mediated response amplitudes (at –60 mV) of control uninfected cells after loading pep2m/G10 for 25 minutes are plotted against those ob-tained from infected cells (infected, 82.8 ± 5.7%; ctrl, 55.3 ± 8.1%; $n = 10$; $p < 0.05$). Right, rectification ($I_{-60\ mV}/I_{+40\ mV}$) of the same cells (infected, 4.66 ± 0.97; ctrl, 1.87 ± 0.15; $n = 10$; $p < 0.001$). (**d**) Normalized simultaneously evoked responses from cells expressing or not expressing GluR4-GFP against the time after forming whole-cell configuration. The experiment was conducted after slices were infected and maintained in normal medium for 36 hours, and subsequently maintained in high Mg^{2+} culture medium for 48 hours. (**e**) Average AMPA-R-mediated synaptic responses obtained immediately (–60 mV, thick trace) and 25 minutes after whole-cell infusion of pep2m/G10 (–60 mV and +40 mV, thin trace) from a pair of infected (GluR4-GFP) and uninfected cells. After infection, slices were kept in normal culture medium for 36 hours followed by high Mg^{2+} culture medium for an additional 48–72 hours. (**f**) Left, residual synaptic AMPA-R-mediated response amplitudes (at –60 mV) after loading pep2m/G10 for 25 minutes of control uninfected cells are plotted against those obtained from infected cells (infected, 69.6 ± 3.9%; ctrl, 65.6 ± 5.9%; $n = 12$; $p = 0.70$). Right, rectification ($I_{-60\ mV}/I_{+40\ mV}$) of the same cells (infected, 1.96 ± 0.14; ctrl, 1.94 ± 0.22; $n = 12$; $p = 0.58$).

for longer periods of time. Indeed, the recently described AMPA receptor cycling[15–19] may be important in the long-term maintenance of activity-induced synaptic plasticity.

Methods

Biochemical analyses. Hippocampal extracts were prepared in homogenization buffer, as described[13]. Expression of AMPA receptor subunits was analyzed by western blot and quantified by chemiluminescence and densitometric scanning of the films under linear exposure conditions. For co-immunoprecipitation experiments, cell extracts were obtained from the CA1 region after viral expression[13]. After reaction with anti-GFP (monoclonal, 4 μg per sample, Boehringer Mannheim, Roche Molecular Biochemicals, Indianapolis, Indiana), anti-GluR1, anti-GluR2 or anti–NR1 antibodies (polyclonal, 1 μg per sample, Chemicon, Temecula, California) at 4°C for 2 hours, the immunocomplex was absorbed onto Protein G Sepharose resin (40 μl; Amersham Pharmacia Biotech, Piscataway, California) at 4°C for 2 hours. Finally the resin was washed three times with homogenization buffer, separated by SDS-PAGE and blotted with anti-GluR4 or anti-GluR1 antibodies (polyclonal, Chemicon). The immunoprecipitation of each subunit by its corresponding antibody was virtually complete (data not shown). To quantify the amount of GluR4-GFP associated with GluR2, we compared the amount of GluR4-GFP precipitated by anti-GluR2 and the amount of GluR4-GFP precipitated by anti-GFP (18.5 ± 6% of GluR4-GFP was associated with GluR2). As a control, the amount of GluR1 immunoprecipitated by anti-GluR2 was about the same as the amount of GluR1 immunoprecipitaed by anti-GluR1 (approximately 100% of GluR1 was associated with GluR2). Immunoblots were quantified as described above.

Constructs of recombinant receptors and expression. Constructs of AMPA receptor subunits tagged with GFP were made as previously described[12]. Briefly, the GFP coding sequence (enhanced GFP, Clontech, Palo Alto, California) was inserted after the predicted signal peptide cleavage site of the corresponding AMPA receptor subunit. GluR4ct-GFP was made by PCR amplification of the GluR4 coding sequence from amino acids 829 to 872, and in-frame ligation into pEGFP-C1 (Clontech). GluR1ct-GFP and GluR2ct-GFP were made by PCR amplification of the GluR1 C-terminus (amino acids 809–889) or GluR2 C-terminus (amino acids 813–862) and in-frame ligation into pEGFP-C1 (Clontech). These constructs were expressed in CA1 neurons in rat hippocampal slices, using Sindbis virus[13]. Slices were prepared, typically from postnatal 5–7 day (P5–7) old animals, immediately infected, and incubated on culture medium and 5% CO_2. For pharmacological experiments (Fig. 3b–e), slices were maintained in culture medium containing drugs, from the

time they were infected with virus. Immunostaining, two-photon imaging, co-immunoprecitation and electrophysiological recording experiments were done approximately 36 hours later unless stated otherwise. Slices were made from P9–10 animals, immediately infected and incubated for 36 hours before electrophysiology (Fig. 5e and f). Slices were also prepared from P5–7 animals, immediately infected and maintained in culture for up to 4.5 days before recordings (Figs. 6 and 7).

Immunohistochemistry for two-photon microscopy. Immunostaining experiments were carried out as described[13] using a mouse monoclonal anti-GFP antibody (Boehringer Mannheim, Roche Molecular Biochemicals) for the detection of GluR4-GFP or a rabbit polyclonal anti-GluR4 antibody (Chemicon) for the detection of endogenous receptors. Antibody incubations were in PBS at 4ºC for 48 hours (primary antibodies) or overnight (secondary antibodies and avidin-Texas Red). Detergents were omitted in all incubations when surface expression was evaluated. GFP and Texas Red fluorescent images were taken with a custom-built two-photon laser scanning microscope[12].

Immunohistochemistry for electron microscopy. Pre-embedding immunogold staining for GluR4-GFP was carried out with mouse anti-GFP (Boehringer Mannheim, Roche Molecular Biochemicals), biotinylated anti-mouse (Sigma, St. Louis, Missouri) and streptavidin-nanogold (Energy Beam Sciences, Agawam, Massachusetts). Antibody incubations were as described above but using 0.8% BSA, 0.1% gelatin (Amersham Pharmacia Biotech) in PBS. Nanogold was enhanced with the gold-enhancement kit from Nanoprobes (Yaphank, New York). Samples were osmicated with 1% OsO_4, dehydrated with a graded series of ethanol and embedded in Epon-Araldite.

Transfection of HEK cells. HEK 293 cells were transfected by GluR4-GFP with Lipofectin reagent (Gibco BRL, Life Technologies, Rockville, Maryland). After 36 hours, recordings were taken from transfected cells with patch pipettes containing Cs-based intracellular solution. The GluR4-GFP-mediated responses were evoked by a brief pulse (5–10 ms) of agonist (kainate, 1 mM) in the presence of cyclothiazide (0.1 mM) and averaged for 8 trials at different holding potentials.

Electrophysiology. Simultaneous whole-cell recordings[45] were obtained from nearby pairs of infected and uninfected CA1 neurons, under visual guidance using fluorescence and transmitted light illumination. The recording chamber was perfused with physiological solution (29 ± 1.5ºC), and unless otherwise stated, contained 119 mM NaCl, 2.5 mM KCl, 4 mM $CaCl_2$, 4 mM $MgCl_2$, 26 mM $NaHCO_3$, 1 mM NaH_2PO_4, 11 mM glucose, 0.1 mM picrotoxin, 10 μM bicuculline, 0.1 mM AP and 2 μM 2-chloroadenosine at pH 7.4, gassed with 5% CO_2/95% O_2. To prevent bursting, 2-chloroadenosine was included. For experiments in which slices were maintained in culture with APV or KN-93 (Fig. 3b–e), these drugs were included during recordings. APV was not included in the bath solution during the experiments that estimated the fraction of silent synapses (Fig. 4). With TTX (1 μM) or high Mg^{2+} (10 mM), only spontaneous miniature responses remained. Patch recording pipettes (4–7 MΩ) were filled with intracellular solutions containing 115 mM cesium methanesulfonate, 20 mM CsCl, 10 mM HEPES, 2.5 mM $MgCl_2$, 4 mM Na_2ATP, 0.4 mM Na_3GTP, 10 mM sodium phosphocreatine, 0.6 mM EGTA and 0.1 mM spermine, at pH 7.25 for current recordings, or 115 mM potassium gluconate, 10 mM HEPES, 2 mM $MgCl_2$, 2 mM MgATP, 2 mM Na_2ATP, 0.3 mM Na_3GTP, and 20 mM KCl, at pH 7.25, for voltage recordings. Whole-cell recordings were made with two Axopatch-1D or Axoclamp 2A amplifiers (Axon Instruments, Foster City, California). The resting membrane potentials (infected, –57.7 ± 1.0 mV; control, –58.0 ± 0.8 mV; $n = 11$; $p = 0.45$) and input resistances (infected, 216 ± 15 MΩ; ctrl, 225 ± 19 MΩ; $n = 11$; $p = 0.37$), measured in current-clamp mode, were similar for infected and non-infected cells. Junction potentials were not corrected. Spontaneous activity was examined with recording chamber perfused with either slice culture medium containing 79% MEM, 20% horse serum, 3 mM L-glutamine, 18.4 mM glucose, 5 mM $NaHCO_3$, 2.26 mM $CaCl_2$, 2.81 mM $MgSO_4$, 30 mM HEPES, 0.07 mM ascorbic acid and 0.17 μM insulin at pH 7.28 ($n = 4$ pairs) or physiological solution containing 2.26 mM Ca^{2+} and 2.81 mM Mg^{2+} ($n = 16$). Similar patterns were found using both solutions. For power spectra, 10–20 periods of 10 seconds were sampled; for each period, a power spectrum (from FFT) and their averages and s.e.m. were calculated. Synaptic responses were evoked by 1 or 2 bipolar electrodes with single voltage pulses (200 μs, up to 20 V). The stimulating electrodes were placed over Schaffer collateral fibers approximately 300–500 μm from the CA1 cells. Synaptic AMPA responses at –60 mV and +40 mV were averaged over 90 trials, and their ratio was used as an index of rectification. Success rate of synaptic transmission was calculated from 200 trials, similar to the method previously described[29]. The peptide pep2m/G10 (KRMKVAKNAQ, Research Genetics, Huntsville, Alabama) was dissolved (2 mM) in Cs-based internal solution. Experiments were done at 22–23°C. Responses within 5 minutes after forming whole-cell configuration and after 25 minutes of loading pep2m/G10 were averaged and compared. All results are reported as mean ± standard error of the mean (s.e.m.), and statistical differences of the means were determined using Wilcoxon non-parametric test unless otherwise stated. Significance was set at $p \leq 0.05$.

Histology. To recover cell morphology, we included biocytin (0.25%) in the intracellular solutions in some experiments. Slices were fixed by immersion in 4% paraformaldehyde in 0.1 M phosphate buffer after recordings for 24 hours, then histologically reacted for biocytin. Infected cells had similar dendritic morphology as control non-infected cells (n = 7 pairs; Fig. 2c). Cells were drawn with the aid of a camera lucida system.

Note: supplementary information on determing relative amounts of GluR1, GluR2 and GluR4 in hippocampal extracts is available on the Nature Neuroscience web site (http://neurosci.nature.com/web_specials/).

Acknowledgements

We thank Song-Hai Shi for help in cloning GluR2-GFP and GluR3-GFP constructs, Nancy Dawkins-Pisani and Tamara Howard for technical assistance, and H. Cline, J. Huang, Z. Mainen, E. Ruthazer and members of the Malinow laboratory for comments and discussions. This study was supported by the NIH, the Alzheimer's Association and the NARSAD Foundation.

Received 12 July; Accepted 13 September 2000

1. Ramon y Cajal, S. *Histologie du System Nerveux de l'Homme et Vertebres* (Instituto Ramon y Cajal, Madrid, 1911).
2. Goodman, C. S. & Shatz, C. J. Developmental mechanisms that generate precise patterns of neuronal connectivity. *Cell* 72 Suppl., 77–98 (1993).
3. O'Brien, R. J. *et al.* Synaptic clustering of AMPA receptors by the extracellular immediate-early gene product Narp. *Neuron* 23, 309–323 (1999).
4. Scheiffele, P., Fan, J., Choih, J., Fetter, R. & Serafini, T. Neuroligin expressed in nonneuronal cells triggers presynaptic development in contacting axons. *Cell* 101, 657–669 (2000).
5. Cline, H. T., Wu, G. Y. & Malinow, R. In vivo development of neuronal structure and function. *Cold Spring Harb. Symp. Quant. Biol.* 61, 95–104 (1996).
6. Dingledine, R., Borges, K., Bowie, D. & Traynelis, S. F. The glutamate receptor ion channels. *Pharmacol. Rev.* 51, 7–61 (1999).
7. Petralia, R. S. *et al.* Selective acquisition of AMPA receptors over postnatal development suggests a molecular basis for silent synapses. *Nat. Neurosci.* 2, 31–36 (1999).
8. Liao, D., Zhang, X., O'Brien, R., Ehlers, M. D. & Huganir, R. L. Regulation of morphological postsynaptic silent synapses in developing hippocampal neurons. *Nat. Neurosci.* 2, 37–43 (1999).
9. Wu, G., Malinow, R. & Cline, H. T. Maturation of a central glutamatergic synapse. *Science* 274, 972–976 (1996).
10. Durand, G. M., Kovalchuk, Y. & Konnerth, A. Long-term potentiation and functional synapse induction in developing hippocampus. *Nature* 381, 71–75 (1996).
11. Isaac, J. T., Crair, M. C., Nicoll, R. A. & Malenka, R. C. Silent synapses during development of thalamocortical inputs. *Neuron* 18, 269–280 (1997).
12. Shi, S. H. *et al.* Rapid spine delivery and redistribution of AMPA receptors after synaptic NMDA receptor activation. *Science* 284, 1811–1816 (1999).
13. Hayashi, Y. *et al.* Driving AMPA receptors into synapses by LTP and CaMKII: requirement for GluR1 and PDZ domain interaction. *Science* 287, 2262–2267 (2000).
14. Constantine-Paton, M. & Cline, H. T. LTP and activity-dependent synaptogenesis: the more alike they are, the more different they become. *Curr. Opin. Neurobiol.* 8, 139–148 (1998).
15. Nishimune, A. *et al.* NSF binding to GluR2 regulates synaptic transmission. *Neuron* 21, 87–97 (1998).

16. Osten, P. *et al.* The AMPA receptor GluR2 C terminus can mediate a reversible, ATP- dependent interaction with NSF and alpha- and beta-SNAPs. *Neuron* 21, 99–110 (1998).
17. Song, I. *et al.* Interaction of the N-ethylmaleimide-sensitive factor with AMPA receptors. *Neuron* 21, 393–400 (1998).
18. Luthi, A. *et al.* Hippocampal LTD expression involves a pool of AMPARs regulated by the NSF-GluR2 interaction. *Neuron* 24, 389–399 (1999).
19. Luscher, C. *et al.* Role of AMPA receptor cycling in synaptic transmission and plasticity. *Neuron* 24, 649–658 (1999).
20. Malinow, R. *et al.* in *Imaging Neurons: A Laboratory Manual* (eds. Yuste, R., Lanni, F. & Konnerth, A) 58.1–58.8 (Cold Spring Harbor Laboratory Press, Cold Spring Harbor, New York, 1999).
21. Verdoorn, T. A., Burnashev, N., Monyer, H., Seeburg, P. H. & Sakmann, B. Structural determinants of ion flow through recombinant glutamate receptor channels. *Science* 252, 1715–1718 (1991).
22. Hestrin, S., Nicoll, R. A., Perkel, D. J. & Sah, P. Analysis of excitatory synaptic action in pyramidal cells using whole-cell recording from rat hippocampal slices. *J. Physiol. (Lond.)* 422, 203–225 (1990).
23. Ben-Ari, Y., Cherubini, E., Corradetti, R. & Gaiarsa, J. L. Giant synaptic potentials in immature rat CA3 hippocampal neurones. *J. Physiol. (Lond.)* 416, 303–325 (1989).
24. Garaschuk, O., Hanse, E. & Konnerth, A. Developmental profile and synaptic origin of early network oscillations in the CA1 region of rat neonatal hippocampus. *J. Physiol. (Lond.)* 507, 219–236 (1998).
25. Palva, J. M. *et al.* Fast network oscillations in the newborn rat hippocampus in vitro. *J. Neurosci.* 20, 1170–1178 (2000).
26. Margrie, T. W., Rostas, J. A. & Sah, P. Presynaptic long-term depression at a central glutamatergic synapse: a role for CaMKII. *Nat. Neurosci.* 1, 378–383 (1998).
27. Lisman, J., Malenka, R. C., Nicoll, R. A. & Malinow, R. Learning mechanisms: the case for CaM-KII. *Science* 276, 2001–2002 (1997).
28. Liao, D. & Malinow, R. Deficiency in induction but not expression of LTP in hippocampal slices from young rats. *Learn. Mem.* 3, 138–149 (1996).
29. Liao, D., Hessler, N. A. & Malinow, R. Activation of postsynaptically silent synapses during pairing-induced LTP in CA1 region of hippocampal slice. *Nature* 375, 400–404 (1995).
30. O'Brien, R. J., Lau, L. F. & Huganir, R. L. Molecular mechanisms of glutamate receptor clustering at excitatory synapses. *Curr. Opin. Neurobiol.* 8, 364–369 (1998).
31. Katz, L. C. & Shatz, C. J. Synaptic activity and the construction of cortical circuits. *Science* 274, 1133–1138 (1996).
32. Ruthazer, E. S. & Stryker, M. P. The role of activity in the development of long-range horizontal connections in area 17 of the ferret. *J. Neurosci.* 16, 7253–7269 (1996).
33. Kim, H. G., Fox, K. & Connors, B. W. Properties of excitatory synaptic events in neurons of primary somatosensory cortex of neonatal rats. *Cereb. Cortex* 5, 148–157 (1995).
34. Isaac, J. T., Nicoll, R. A. & Malenka, R. C. Evidence for silent synapses: implications for the expression of LTP. *Neuron* 15, 427–434 (1995).
35. Galli, L. & Maffei, L. Spontaneous impulse activity of rat retinal ganglion cells in prenatal life. *Science* 242, 90–91 (1988).
36. Weliky, M. & Katz, L. C. Correlational structure of spontaneous neuronal activity in the developing lateral geniculate nucleus in vivo. *Science* 285, 599–604 (1999).
37. Bliss, T. V. & Collingridge, G. L. A synaptic model of memory: long-term potentiation in the hippocampus. *Nature* 361, 31–39 (1993).
38. Zamanillo, D. *et al.* Importance of AMPA receptors for hippocampal synaptic plasticity but not for spatial learning. *Science* 284, 1805–1811 (1999).
39. Rao, A. & Craig, A. M. Activity regulates the synaptic localization of the NMDA receptor in hippocampal neurons. *Neuron* 19, 801–812 (1997).
40. Turrigiano, G. G., Leslie, K. R., Desai, N. S., Rutherford, L. C. & Nelson, S. B. Activity-dependent scaling of quantal amplitude in neocortical neurons. *Nature* 391, 892–896 (1998).
41. Lissin, D. V. *et al.* Activity differentially regulates the surface expression of synaptic AMPA and NMDA glutamate receptors. *Proc. Natl. Acad. Sci. USA* 95, 7097–7102 (1998).
42. Gomperts, S. N., Carroll, R., Malenka, R. C. & Nicoll, R. A. Distinct roles for ionotropic and metabotropic glutamate receptors in the maturation of excitatory synapses. *J. Neurosci.* 20, 2229–2237 (2000).
43. Bekkers, J. M. & Stevens, C. F. Presynaptic mechanism for long-term potentiation in the hippocampus. *Nature* 346, 724–729 (1990).
44. Liu, S. Q. & Cull-Candy, S. G. Synaptic activity at calcium-permeable AMPA receptors induces a switch in receptor subtype. *Nature* 405, 454–458 (2000).
45. Zhu, J. J. Maturation of layer 5 neocortical pyramidal neurons: amplifying salient layer 1 and layer 4 inputs by Ca^{2+} action potentials in adult rat tuft dendrites. *J. Physiol. (Lond.)* 526, 571–587 (2000).